

## Quantum Kibble-Zurek Mechanism in a Spin-1 Bose-Einstein Condensate

M. Anquez, B. A. Robbins, H. M. Bharath, M. Boguslawski, T. M. Hoang, and M. S. Chapman\*

*School of Physics, Georgia Institute of Technology, Atlanta, Georgia 30332, USA*

(Received 18 December 2015; published 12 April 2016)

The dynamics of a quantum phase transition are explored using slow quenches from the polar to the broken-axisymmetry phases in a small spin-1 ferromagnetic Bose-Einstein condensate. Measurements of the evolution of the spin populations reveal a power-law scaling of the temporal onset of excitations versus quench speed as predicted from quantum extensions of the Kibble-Zurek mechanism. The satisfactory agreement of the measured scaling exponent with the analytical theory and numerical simulations provides experimental confirmation of the quantum Kibble-Zurek model.

DOI: [10.1103/PhysRevLett.116.155301](https://doi.org/10.1103/PhysRevLett.116.155301)

Symmetry-breaking continuous phase transitions play important roles in many areas of physics including cosmology, particle physics, and condensed matter. When a system is quenched across the critical point of a continuous phase transition, the time scale characterizing the dynamics diverges, and subsequent nonadiabatic evolution generally gives rise to topological defect excitations. The Kibble-Zurek mechanism (KZM) provides a general theory for understanding the nonequilibrium dynamics of these systems and predicts a universal power-law scaling of the excitations as a function of the quench rate with an exponent that is simply related to the equilibrium critical exponents [1–5]. The KZM was first introduced by Kibble in his study on the topology of cosmic domains and strings in the early universe [1,2]; it was later extended by Zurek [3–5] who suggested applying these symmetry breaking ideas to laboratory accessible condensed matter systems, including superconductors and superfluids. This seminal work inspired a host of theoretical [6–13] and experimental [14–34] investigations of KZ scaling in thermodynamic (finite temperature) transitions; for a recent review, see [35].

There is much current interest in extending the KZM to continuous quantum phase transitions (QPTs), which are zero temperature transitions driven by Heisenberg quantum fluctuations rather than thermal fluctuations [36,37]. In these transitions, a qualitative change in the ground state occurs when a parameter in the Hamiltonian is varied across the quantum critical point (QCP) at zero temperature. There have been many theoretical proposals for observing the KZM in a quantum phase transition [37–49]; however, thus far, only two experiments have investigated the scaling of excitations with quench speed [50,51] in a QPT, both using the Mott insulator to Bose-Hubbard superfluid (SF) transition in optical lattices. In [50], the excitations of a condensate were measured versus quench speeds in a 3D lattice quenched into the SF phase, and in [51], the temporal growth of the coherence length was measured versus quench speed into the SF phase for different lattice dimensionalities. Power law scaling was

observed in both experiments, but the measured exponents did not agree with KZM analyses of the critical exponents [35,52]. Furthermore, the measured dynamics in [51] show complex behavior beyond power-law scaling that indicate that the KZM model does not adequately capture the underlying physics or, at best, could only be observed in unrealistically slow quenches [52]. A particular challenge for these experiments is that with the exception of the 1D lattice investigated in [51], quantum simulations of the realistic experimental conditions are beyond current capabilities. Hence, there is strong motivation for additional experimental investigations, ideally in simpler quantum systems that permit direct comparison to theory.

Several theoretical investigations have suggested that the polar ( $P$ ) to broken-axisymmetry (BA) quantum phase transition in spin-1 condensates would be a promising platform for verifying the quantum KZM [44,45,53–56]. Although excitations following fast quenches have been studied in a number of spinor Bose-Einstein condensate (BEC) experiments [57–62] (including a recent paper that observed the scaling of excitations versus quench depth in a two-component BEC [63]), the scaling of the spin excitations versus quench speed predicted by the KZM has not been measured.

In this Letter, we investigate the KZM using small spin-1  $^{87}\text{Rb}$  condensates by measuring the evolution of the spin populations during slow quenches from the polar phase. The temporal onset of spin excitations show a power-law dependence versus the quench speed with an exponent that is within 15% of the prediction of the analytical KZM model and in good agreement with quantum simulations of the quench dynamics incorporating the measured experimental conditions. A distinguishing feature of our KZM investigation is that, unlike in spatially extended systems where the KZM is manifest in topological defects, the excitations in our experiment are constrained to the temporal evolution of the spin populations because spin domain formation is suppressed for small condensates. This simplifies the complexity of the system and permits

accurate quantum simulations to be performed using realistic experimental parameters.

The spin dynamics of a small spin-1 BEC in a magnetic field along the  $z$  axis can be described by the Hamiltonian:  $\hat{H} = \tilde{c}\hat{S}^2 - (q/2)\hat{Q}_z$ . The first term describes the spin interactions, where  $\tilde{c}$  is the spin-dependent elastic collision coefficient related to the  $s$ -wave scattering lengths for collisions between pairs of atoms ( $\tilde{c} < 0$  for ferromagnetic condensates), and  $\hat{S}^2 = \hat{S}_x^2 + \hat{S}_y^2 + \hat{S}_z^2$  is the total spin vector operator. The second term describes the quadratic Zeeman energy per particle.  $\hat{Q}_z$  is proportional to the spin-1 quadrupole moment,  $\hat{Q}_{zz}$  [61], and  $q = q_z B^2$  is the quadratic Zeeman energy per particle, where  $B$  is the magnitude of the magnetic field and  $q_z \approx 71.6 \text{ Hz/G}^2$  (hereafter,  $h = 1$ ). In terms of the mean-field expectation values, the spin energy is

$$H = \frac{c}{2}S^2 - \frac{q}{2}Q_z, \quad (1)$$

where  $c \propto \tilde{c}$  is the spinor dynamical rate and  $Q_z = 2\rho_0 - 1$ , with  $\rho_0$  being the fractional population in the  $|F = 1, m_F = 0\rangle$  state. The states of the system can be represented on the  $\{S_\perp, Q_\perp, Q_z\}$  unit sphere, where  $S_\perp^2 = S_x^2 + S_y^2$  and  $Q_\perp^2 = Q_{xz}^2 + Q_{yz}^2$  [61], as shown in Fig. 1.

The quantum critical point between the  $P$  and BA phases occurs at  $q_c = 2|c|$ . Using Bogoliubov theory, it can be

shown that the BA phase ( $q < q_c$ ) ground state has three excitation modes [64]. Two are gapless modes (in the long wavelength limit) which arise from the  $SO(2)$  symmetry breaking as predicted by the Goldstone theorem [65]; the third mode has a nonzero eigenvalue, corresponding to the energy gap between the ground and first excited state [see Fig. 1(a)]

$$\Delta = \sqrt{q_c^2 - q^2} \sim |q_c - q|^{1/2}, \quad (2)$$

where the approximation is valid near  $q = q_c$ .

A universal feature of QPTs is that, close to the critical point, the properties of the system are uniquely described by critical exponents determining the functional form of the energy gap as a function of the parameters of the Hamiltonian:  $\Delta \sim |g_c - g|^{z\nu}$ , where  $z, \nu$  are the critical exponents,  $g$  is the tuning parameter, and  $g_c$  is the critical point of the system [36]. Comparing to Eq. (2) shows that  $z\nu = 1/2$  for the spin-1 system.

Because the energy gap  $\Delta$  vanishes at the critical point (ignoring finite-size effects), the system cannot cross the critical point adiabatically. The utility of the KZM is that it provides a universal prescription for quantifying the dynamical excitation based on the exponents  $z, \nu$  that govern the equilibrium behavior of the system [3,38,45,66]. As illustrated in Fig. 1(b), two characteristic time scales can be compared to explain the behavior of the system initialized in the ground state of one phase as it is driven across the QCP. The first is the reaction time of the system to changes in the Hamiltonian, which is inversely proportional to the energy gap  $\Delta$ . The second is  $\Delta/\dot{\Delta}$ , which describes how fast the system is driven through the critical point. In our experiment, the system is driven from the polar to the BA phase. Close to the critical point, the reaction time is too large for the evolution to be adiabatic, and the evolution shifts to an impulse regime where the system remains frozen in the polar ground state in the mean-field approximation. When the two time scales become comparable again, the system unfreezes and is now in an excited state. The dynamics resume and the system is able to adiabatically evolve towards the BA ground state.

The freeze out time  $\hat{t}$  between the crossing of the critical point and the recovery of adiabatic evolution is a function of the ramp speed and can be found from  $\Delta^{-1}(\hat{t}) = \Delta/\dot{\Delta}|_{t=\hat{t}}$ . For the case of linear ramps of the control parameter of the Hamiltonian ( $q$ , in our case) in a quench time  $\tau_Q$ , then  $\dot{q} \propto \tau_Q^{-1}$  and the power-law relation  $\hat{t} \propto \tau_Q^{\nu z/(1+\nu z)} = \tau_Q^\alpha$ , where  $\alpha = 1/3$ , is obtained (see Supplemental Material [67]). Introducing the dimensionless ratio  $\tilde{q} = q/|c|$  and defining  $\hat{q}$  as the change in  $\tilde{q}$  between the crossing of the critical point and the resuming of dynamics, a power law scaling can also be derived for  $\hat{q}$  using the same approach as for  $\hat{t}$ , which results in  $\hat{q} \sim \tilde{\tau}_Q^{(-1/1+\nu z)} = \tilde{\tau}_Q^\beta$ , where  $\beta = -2/3$  and  $\tilde{\tau}_Q$  is the inverse of the rate of change of  $\tilde{q}$  at the critical point.

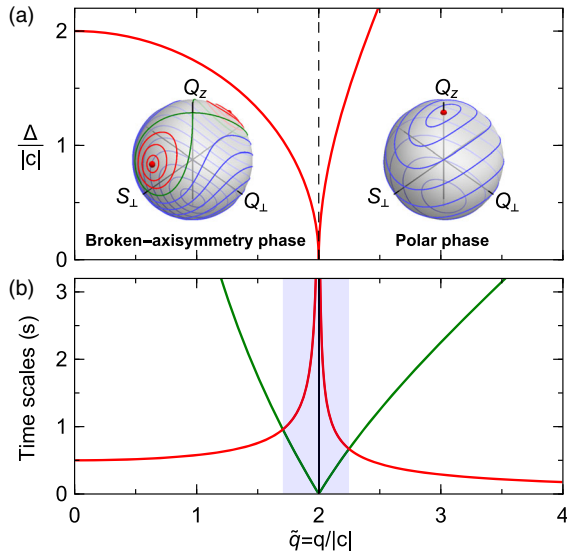


FIG. 1. Concept: (a) The energy gap  $\Delta$  between the ground state and first excited state is plotted as a function of the quadratic Zeeman energy  $q$  (in units of  $|c|$ ). The gap vanishes at the critical point  $q_c = 2|c|$ , shown by the vertical dashed line. The spheres show the spin-nematic phase space for different values of  $q$ : (left) broken-axisymmetry phase ( $q < 2|c|$ ) and (right) polar phase ( $q > 2|c|$ ). The ground state in each phase is indicated with red dots. (b) The “freeze-out” region for a given ramp speed (blue shaded) is determined by the intersection of the minimum response time (red) and the effective speed of the ramp (green). See text for details.

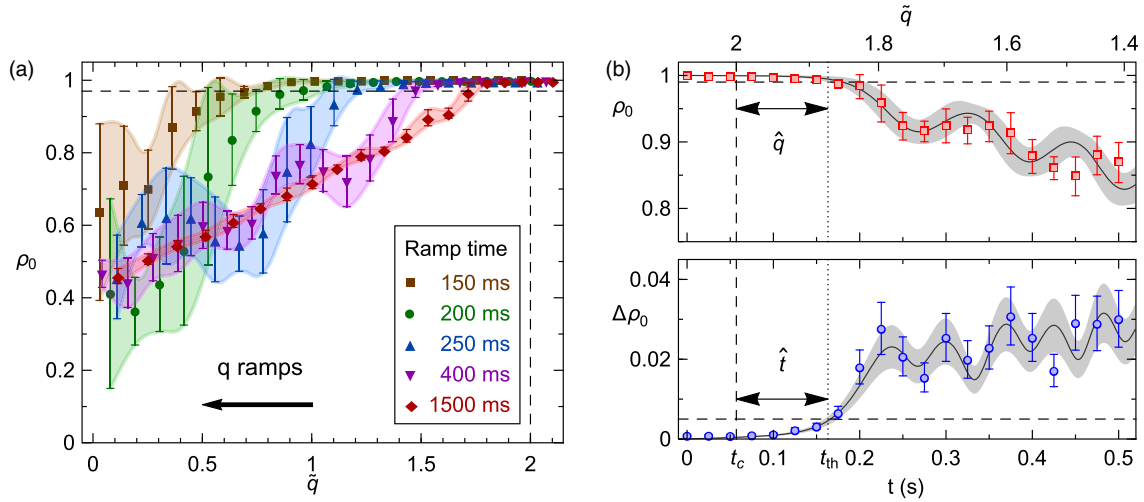


FIG. 2. Quench dynamics: (a) Measurements of  $\rho_0$  for different ramp times as a function of  $\tilde{q} = q/|c|$ . The ramp times shown correspond to the duration to ramp the magnetic field from  $\tilde{q} = 2.2$  to  $\tilde{q} = 0$ . The longer ramps show evolution after a smaller change in  $\tilde{q}$  than the shorter ramps. For the latter, the system stays frozen in the polar phase ground state ( $\rho_0 = 1$ ) until a larger change in  $\tilde{q}$ , as expected from the KZM. The horizontal and vertical dashed lines indicate the  $\rho_0$  threshold and the critical point, respectively. (b) Measurements of  $\rho_0$  (red squares) and its standard deviation  $\Delta\rho_0$  (blue circles) during a typical experimental run where the magnetic field is slowly ramped down through the critical point such that the  $q$  decreases linearly. The thresholds used to determine when the system “unfreezes” are shown as horizontal dashed lines. The system shows good agreement with simulations (gray curves and envelopes showing  $\pm 1$  standard deviation) for long evolution times beyond the freeze-out period. The top axis shows  $\tilde{q}$ , with the vertical dashed line at  $\tilde{q} = 2$  marking the critical point. The dotted line indicates when the system crosses the determined threshold.

The experiments use small spin-1  $^{87}\text{Rb}$  atomic Bose condensates in the  $F = 1$  hyperfine state confined in an optical dipole trap. The condensates are initialized in the  $m_F = 0$  state in a high magnetic field, which is the polar ground state [see Fig. 1(a), right]. The condensates are quenched across the QCP at different speeds, and the onset time (and corresponding value of  $q$ ) for excitations from the polar ground state are determined from the time evolution of the mean value spin population  $\rho_0$  and the fluctuation  $\Delta\rho_0$ . In Fig. 2(a), the results from several ramps are shown. For each of these ramps, the field is first lowered quickly to  $q_0 = 2.2|c|$ , and then ramped according to  $q(t) = q_0 - t/\tau_Q$  for a range of  $\tau_Q$  values. For asymptotically slow ramps, the population  $\rho_0$  should adiabatically follow the ground state value  $\rho_{0,\text{GS}} = 1/2 + q/4|c|$  for  $q < q_c = 2|c|$ . From the data in Fig. 2(a), it is clear that the population lags the ground state value by an amount that increases for faster ramps, indicating the nonadiabatic crossing of the QCP.

The determinations of  $\hat{t}$  and  $\hat{q}$  are shown in Fig. 2(b), which shows both  $\rho(t)$  and  $\Delta\rho_0(t)$  for a typical quench. To determine when the system “unfreezes,” thresholds of  $\rho_0 = 0.99$  and  $\Delta\rho_0 = 0.005$  are used. As pointed out in [45], the exponent is insensitive to the choice of the exact thresholds. The freeze-out time is  $\hat{t} = t_{th} - t_c$ , where  $t_c$  is the time the system crosses the critical point and  $t_{th}$  is where  $\rho_0$  and  $\Delta\rho_0$  reach their respective thresholds.  $\hat{q}$  is determined similarly to  $\hat{t}$ , and is given by  $\hat{q} = \tilde{q}(t_{th}) - \tilde{q}(t_c)$ . The use of  $\tilde{q}$  allows us to incorporate the effect of the finite lifetime of the condensate ( $\sim 2$  s) in the data analysis. The

value  $q/|c|$  is affected by the reduction of density due to the finite lifetime of the condensate, as the spin interaction energy depends on the density and atom number as  $c(t) \propto n(t) \propto N(t)^{2/5}$  (see Supplemental Material [67]), which we account for by using  $\tilde{q} = q(t)/|c(t)|$ .

In order to be able to extract accurate values for  $\hat{t}$  and  $\hat{q}$ , it is necessary to make a careful determination of  $q_c = 2|c|$ . This is achieved by preparing the system in the polar ground state and measuring the onset of fluctuations in  $\rho_0$  following a fast quench from a high field to a final field value in the neighborhood of the critical field,  $B_c$ . For final field values above  $B_c$ , the subsequent fluctuations are negligible, but there is a sharp onset of fluctuations below  $B_c$ . Using this approach,  $B_c$  is determined with an uncertainty as low as 2 mG (Supplemental Material [67]).

To determine the scaling of the excitations as a function of ramp speed, the values of  $\hat{q}$  are plotted versus  $\tilde{\tau}_Q$  as in Fig. 3. The data are fit to a power law, which reveals good agreement, except for the slowest ramps ( $\tilde{\tau}_Q > 1.5$ ), which start to deviate from the fit. This is likely due to the large amount of atom loss in this regime. The inset in Fig. 3 shows the same data in a log-log plot along with a linear fit of the data between  $0.04 < \tilde{\tau}_Q < 1.5$ . This fit yields the power law exponent  $\beta = -0.80(8)$ , where the quantity in parentheses is 1 standard deviation. The data are compared with simulations matching the experiment conditions (gray shaded region), and the agreement is satisfactory. In particular, the power law exponent determined from the simulations is  $\beta = -0.79(7)$ . The experiment was repeated

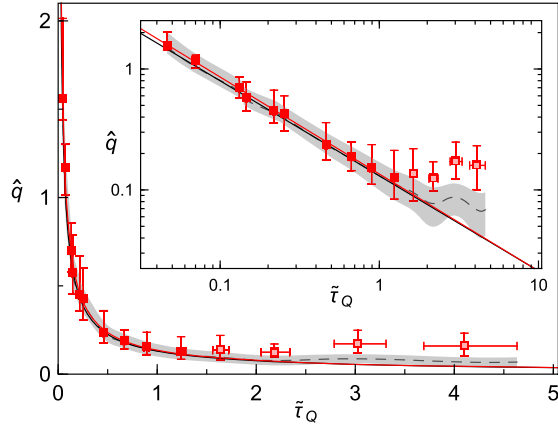


FIG. 3. Power law fit:  $\hat{q}$  data (red squares) and simulations (dashed line with  $\pm 1$  standard deviation envelope) plotted with respect to the characteristic ramp time  $\tilde{\tau}_Q$ . The red and black solid lines correspond to fits to the data and simulations, respectively. The inset shows a linear fit to the log of the data for  $\tilde{\tau}_Q < 1.5$  (solid markers), yielding a scaling exponent of  $-0.80(8)$ .

multiple times over several months, and the results are summarized in Fig. 4. The scaling exponents were determined from analyzing both  $\rho_0$  and  $\Delta\rho_0$ ; the latter are shown as blue markers (see Supplemental Material [67] for results from all data sets). The fourth data set used a different trap geometry—an elongated cigar-shaped trap, which benefits from a longer lifetime of  $\sim 15$  s. Even though the condensate was no longer in the single mode approximation, no spin domains were detected before the system crossed the thresholds used to determine the freeze-out time, and the measured  $\beta = -0.80(10)$  is also in good agreement with simulations using the experimental settings.

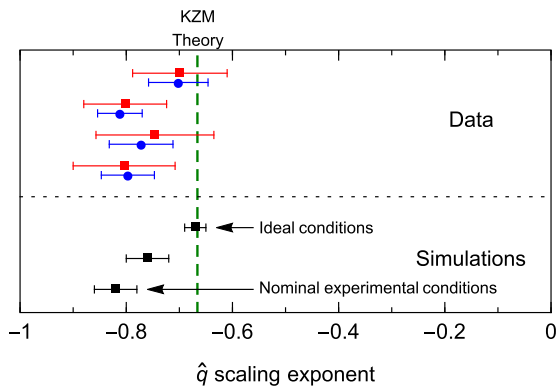


FIG. 4. Summary of scaling exponents: The red squares and blue circles indicate the scaling exponents for data sets analyzed using  $\rho_0$  and  $\Delta\rho_0$  as thresholds, respectively. The results from Fig. 3 correspond to the second data set. The shaded boxes show the results from simulations performed with the experimental conditions corresponding to the given data set. Additional simulations are represented by black squares, showing, from top to bottom: ideal conditions, fast ramps starting at a high magnetic field, and nominal experimental conditions. The dashed vertical line indicates the value predicted by the KZM theory.

The observed scaling exponents are self-consistent (within experimental uncertainty) and agree well with the simulations. They are, however, slightly more negative than the  $-2/3$  value derived above. To investigate this discrepancy, we have performed simulations varying a wide range of parameters including atom number, ramp speeds, initial magnetic fields, and condensate lifetime (Supplemental Material [67]).

Simulations performed in ideal conditions (infinite condensate lifetime, high initial magnetic field, and large number of atoms) yield  $\beta = -0.67(2)$  for very long ramps ( $\tilde{\tau}_Q > 2$ ), in excellent agreement with the value of  $-2/3$  predicted by the KZM (see Fig. 4). However, for the faster ramps that we can measure due to the finite lifetime of the system, the simulations of the ideal case yield a more negative result with  $\beta = -0.76(4)$ . The restriction of the simple theory to the slowest ramps was pointed out in [45]. A second consequence of the lifetime of the condensate is that it prevents starting the magnetic field ramps at a value much higher than the critical point, since a large number of atoms would be lost by the time the system crossed the critical point. A compromise is reached experimentally by starting with a fast drop from a high field ( $q = 17.1q_c$ ) to a field closer to the critical point ( $q = 1.1q_c$ ), followed by slower ramps through the critical point. When we include this experimental step in the simulations, we get  $\beta = -0.82(4)$ , which agrees with the experimental results. From our simulations, the effects of atom loss are not important in the range of ramps that are used to determine the scaling exponent.

In summary, we have observed the Kibble-Zurek mechanism in spin-1 BEC quantum phase transition by measuring the excitations as a function of the quench speed across the quantum critical point. The results show power-law scaling of the onset of the excitations that are in agreement with theoretical predictions and, thus, provide experimental confirmation of the KZM extended to quantum phase transitions. In the future, it should be possible to explore finite size (quantum) modifications to the KZM in the spin-1 system by varying the system size; simulations performed for different numbers of atoms (holding all other parameters constant) indicate that these effects should be observable in our experiments.

We would like to thank Christopher Hamley and Benjamin Land for their early contributions to the theory and simulations, and we acknowledge support from the National Science Foundation (Grant No. NSF PHYS-1506294).

\*mchapman@gatech.edu

- [1] T. W. B. Kibble, Topology of cosmic domains and strings, *J. Phys. A* **9**, 1387 (1976).
- [2] T. W. B. Kibble, Some implications of a cosmological phase transition, *Phys. Rep.* **67**, 183 (1980).

- [3] W. H. Zurek, Cosmological experiments in superfluid helium?, *Nature (London)* **317**, 505 (1985).
- [4] W. H. Zurek, Cosmic strings in laboratory superfluids and the topological remnants of other phase transitions, *Acta Phys. Pol. B* **24**, 1301 (1993).
- [5] W. H. Zurek, Cosmological experiments in condensed matter systems, *Phys. Rep.* **276**, 177 (1996).
- [6] P. Laguna and W. H. Zurek, Density of Kinks after a Quench: When Symmetry Breaks, How Big are the Pieces?, *Phys. Rev. Lett.* **78**, 2519 (1997).
- [7] P. Laguna and W. H. Zurek, Critical dynamics of symmetry breaking: Quenches, dissipation, and cosmology, *Phys. Rev. D* **58**, 085021 (1998).
- [8] A. Yates and W. H. Zurek, Vortex Formation in Two Dimensions: When Symmetry Breaks, How Big are the Pieces?, *Phys. Rev. Lett.* **80**, 5477 (1998).
- [9] J. R. Anglin and W. H. Zurek, Vortices in the Wake of Rapid Bose-Einstein Condensation, *Phys. Rev. Lett.* **83**, 1707 (1999).
- [10] J. Dziarmaga, P. Laguna, and W. H. Zurek, Symmetry Breaking with a Slant: Topological Defects after an Inhomogeneous Quench, *Phys. Rev. Lett.* **82**, 4749 (1999).
- [11] N. D. Antunes, L. M. A. Bettencourt, and W. H. Zurek, Vortex String Formation in a 3D U(1) Temperature Quench, *Phys. Rev. Lett.* **82**, 2824 (1999).
- [12] G. J. Stephens, E. A. Calzetta, B. L. Hu, and S. A. Ramsey, Defect formation and critical dynamics in the early universe, *Phys. Rev. D* **59**, 045009 (1999).
- [13] G. J. Stephens, L. M. A. Bettencourt, and W. H. Zurek, Critical Dynamics of Gauge Systems: Spontaneous Vortex Formation in 2D Superconductors, *Phys. Rev. Lett.* **88**, 137004 (2002).
- [14] I. Chuang, R. Durrer, N. Turok, and B. Yurke, Cosmology in the laboratory: Defect dynamics in liquid crystals, *Science* **251**, 1336 (1991).
- [15] M. J. Bowick, L. Chandar, E. A. Schiff, and A. M. Srivastava, The cosmological Kibble mechanism in the laboratory: String formation in liquid crystals, *Science* **263**, 943 (1994).
- [16] P. C. Hendry, N. S. Lawson, R. A. M. Lee, P. V. E. McClintock, and C. D. H. Williams, Generation of defects in superfluid  $^4\text{He}$  as an analogue of the formation of cosmic strings, *Nature (London)* **368**, 315 (1994).
- [17] V. M. H. Ruutu, V. B. Eltsov, A. J. Gill, T. W. B. Kibble, M. Krusius, Yu. G. Makhlin, B. Plačaiš, G. E. Volovik, and Wen Xu, Vortex formation in neutron-irradiated superfluid  $^3\text{He}$  as an analogue of cosmological defect formation, *Nature (London)* **382**, 334 (1996).
- [18] C. Bäuerle, Y. M. Bunkov, S. N. Fisher, H. Godfrin, and G. Pickett, Laboratory simulation of cosmic string formation in the early Universe using superfluid  $^3\text{He}$ , *Nature (London)* **382**, 332 (1996).
- [19] S. Ducci, P. L. Ramazza, W. González-Viñas, and F. T. Arecchi, Order Parameter Fragmentation after a Symmetry-Breaking Transition, *Phys. Rev. Lett.* **83**, 5210 (1999).
- [20] R. Carmi, E. Polturak, and G. Koren, Observation of Spontaneous Flux Generation in a Multi-Josephson-Junction Loop, *Phys. Rev. Lett.* **84**, 4966 (2000).
- [21] A. Maniv, E. Polturak, and G. Koren, Observation of Magnetic Flux Generated Spontaneously During a Rapid Quench of Superconducting Films, *Phys. Rev. Lett.* **91**, 197001 (2003).
- [22] A. Monaco, A. I. Chumakov, Y.-Z. Yue, G. Monaco, L. Comez, D. Fioretto, W. A. Crichton, and R. Rüffer, Density of Vibrational States of a Hyperquenched Glass, *Phys. Rev. Lett.* **96**, 205502 (2006).
- [23] T. Donner, S. Ritter, T. Bourdel, A. Öttl, M. Köhl, and T. Esslinger, Critical behavior of a trapped interacting Bose gas, *Science* **315**, 1556 (2007).
- [24] D. R. Scherer, C. N. Weiler, T. W. Neely, and B. P. Anderson, Vortex Formation by Merging of Multiple Trapped Bose-Einstein Condensates, *Phys. Rev. Lett.* **98**, 110402 (2007).
- [25] C. N. Weiler, T. W. Neely, D. R. Scherer, A. S. Bradley, M. J. Davis, and B. P. Anderson, Spontaneous vortices in the formation of Bose-Einstein condensates, *Nature (London)* **455**, 948 (2008).
- [26] A. del Campo, G. De Chiara, G. Morigi, M. B. Plenio, and A. Retzker, Structural Defects in Ion Chains by Quenching the External Potential: The Inhomogeneous Kibble-Zurek Mechanism, *Phys. Rev. Lett.* **105**, 075701 (2010).
- [27] K. Pyka, J. Keller, H. Partner, R. Nigmatullin, T. Burgermeister, D. Meier, K. Kuhlmann, A. Retzker, M. Plenio, W. H. Zurek *et al.*, Topological defect formation and spontaneous symmetry breaking in ion Coulomb crystals, *Nat. Commun.* **4**, 2291 (2013).
- [28] S. Ejtemaee and P. C. Haljan, Spontaneous nucleation and dynamics of kink defects in zigzag arrays of trapped ions, *Phys. Rev. A* **87**, 051401 (2013).
- [29] S. Ulm, J. Roßnagel, G. Jacob, C. Degünther, S. T. Dawkins, U. G. Poschinger, R. Nigmatullin, A. Retzker, M. B. Plenio, F. Schmidt-Kaler *et al.*, Observation of the Kibble-Zurek scaling law for defect formation in ion crystals, *Nat. Commun.* **4**, 2290 (2013).
- [30] G. Lamporesi, S. Donadello, S. Serafini, F. Dalfovo, and G. Ferrari, Spontaneous creation of Kibble-Zurek solitons in a Bose-Einstein condensate, *Nat. Phys.* **9**, 656 (2013).
- [31] L. Corman, L. Chomaz, T. Bienaimé, R. Desbuquois, C. Weitenberg, S. Nascimbene, J. Dalibard, and J. Beugnon, Quench-Induced Supercurrents in an Annular Bose Gas, *Phys. Rev. Lett.* **113**, 135302 (2014).
- [32] V. I. Yukalov, A. N. Novikov, and V. S. Bagnato, Realization of inverse Kibble-Zurek scenario with trapped Bose gases, *Phys. Lett. A* **379**, 1366 (2015).
- [33] N. Navon, A. L. Gaunt, R. P. Smith, and Z. Hadzibabic, Critical dynamics of spontaneous symmetry breaking in a homogeneous Bose gas, *Science* **347**, 167 (2015).
- [34] S. Deutschländer, P. Dillmann, G. Maret, and P. Keim, Kibble-Zurek mechanism in colloidal monolayers, *Proc. Natl. Acad. Sci. U.S.A.* **112**, 6925 (2015).
- [35] A. del Campo and W. H. Zurek, Universality of phase transition dynamics: Topological defects from symmetry breaking, *Int. J. Mod. Phys. A* **29**, 1430018 (2014).
- [36] S. Sachdev, *Quantum Phase Transitions* (Cambridge University Press, Cambridge, England, 1999).
- [37] J. Dziarmaga, Dynamics of a quantum phase transition and relaxation to a steady state, *Adv. Phys.* **59**, 1063 (2010).
- [38] W. H. Zurek, U. Dorner, and P. Zoller, Dynamics of a Quantum Phase Transition, *Phys. Rev. Lett.* **95**, 105701 (2005).
- [39] J. Dziarmaga, Dynamics of a Quantum Phase Transition: Exact Solution of the Quantum Ising Model, *Phys. Rev. Lett.* **95**, 245701 (2005).

- [40] A. Polkovnikov, Universal adiabatic dynamics in the vicinity of a quantum critical point, *Phys. Rev. B* **72**, 161201 (2005).
- [41] B. Damski and W. H. Zurek, Adiabatic-impulse approximation for avoided level crossings: From phase-transition dynamics to Landau-Zener evolutions and back again, *Phys. Rev. A* **73**, 063405 (2006).
- [42] R. W. Cherng and L. S. Levitov, Entropy and correlation functions of a driven quantum spin chain, *Phys. Rev. A* **73**, 043614 (2006).
- [43] M. Uhlmann, R. Schützhold, and U. R. Fischer, Vortex Quantum Creation and Winding Number Scaling in a Quenched Spinor Bose Gas, *Phys. Rev. Lett.* **99**, 120407 (2007).
- [44] A. Lamacraft, Quantum Quenches in a Spinor Condensate, *Phys. Rev. Lett.* **98**, 160404 (2007).
- [45] B. Damski and W. H. Zurek, Dynamics of a Quantum Phase Transition in a Ferromagnetic Bose-Einstein Condensate, *Phys. Rev. Lett.* **99**, 130402 (2007).
- [46] A. Fubini, G. Falci, and A. Osterloh, Robustness of adiabatic passage through a quantum phase transition, *New J. Phys.* **9**, 134 (2007).
- [47] W. H. Zurek, Causality in Condensates: Gray Solitons as Relics of BEC Formation, *Phys. Rev. Lett.* **102**, 105702 (2009).
- [48] A. Bermudez, D. Patane, L. Amico, and M. A. Martin-Delgado, Topology-Induced Anomalous Defect Production by Crossing a Quantum Critical Point, *Phys. Rev. Lett.* **102**, 135702 (2009).
- [49] A. Bermudez, L. Amico, and M. A. Martin-Delgado, Dynamical delocalization of Majorana edge states by sweeping across a quantum critical point, *New J. Phys.* **12**, 055014 (2010).
- [50] D. Chen, M. White, C. Borries, and B. DeMarco, Quantum Quench of an Atomic Mott Insulator, *Phys. Rev. Lett.* **106**, 235304 (2011).
- [51] S. Braun, M. Friesdorf, S. S. Hodgman, M. Schreiber, J. P. Ronzheimer, A. Riera, M. del Rey, I. Bloch, J. Eisert, and U. Schneider, Emergence of coherence and the dynamics of quantum phase transitions, *Proc. Natl. Acad. Sci. U.S.A.* **112**, 3641 (2015).
- [52] J. Dziarmaga and W. H. Zurek, Quench in the 1D Bose-Hubbard model: Topological defects and excitations from the Kosterlitz-Thouless phase transition dynamics, *Sci. Rep.* **4**, 5950 (2014).
- [53] B. Damski and W. H. Zurek, How to fix a broken symmetry: quantum dynamics of symmetry restoration in a ferromagnetic Bose-Einstein condensate, *New J. Phys.* **10**, 045023 (2008).
- [54] H. Saito, Y. Kawaguchi, and M. Ueda, Kibble-Zurek mechanism in a quenched ferromagnetic Bose-Einstein condensate, *Phys. Rev. A* **76**, 043613 (2007).
- [55] H. Saito, Y. Kawaguchi, and M. Ueda, Kibble-Zurek mechanism in a trapped ferromagnetic Bose-Einstein condensate, *J. Phys. Condens. Matter* **25**, 404212 (2013).
- [56] B. Damski and W. H. Zurek, Quantum phase transition in space in a ferromagnetic spin-1 Bose-Einstein condensate, *New J. Phys.* **11**, 063014 (2009).
- [57] M.-S. Chang, C. D. Hamley, M. D. Barrett, J. A. Sauer, K. M. Fortier, W. Zhang, L. You, and M. S. Chapman, Observation of Spinor Dynamics in Optically Trapped  $^{87}\text{Rb}$  Bose-Einstein Condensates, *Phys. Rev. Lett.* **92**, 140403 (2004).
- [58] L. E. Sadler, J. M. Higbie, S. R. Leslie, M. Vengalattore, and D. M. Stamper-Kurn, Spontaneous symmetry breaking in a quenched ferromagnetic spinor Bose-Einstein condensate, *Nature (London)* **443**, 312 (2006).
- [59] C. Klempt, O. Topic, G. Gebreyesus, M. Scherer, T. Henninger, P. Hyllus, W. Ertmer, L. Santos, and J. J. Arlt, Parametric Amplification of Vacuum Fluctuations in a Spinor Condensate, *Phys. Rev. Lett.* **104**, 195303 (2010).
- [60] C. Gross, H. Strobel, E. Nicklas, T. Zibold, N. Bar-Gill, G. Kurizki, and M. K. Oberthaler, Atomic homodyne detection of continuous-variable entangled twin-atom states, *Nature (London)* **480**, 219 (2011).
- [61] C. D. Hamley, C. S. Gerving, T. M. Hoang, E. M. Bookjans, and M. S. Chapman, Spin-nematic squeezed vacuum in a quantum gas, *Nat. Phys.* **8**, 305 (2012).
- [62] C. S. Gerving, T. M. Hoang, B. J. Land, M. Anquez, C. D. Hamley, and M. S. Chapman, Non-equilibrium dynamics of an unstable quantum pendulum explored in a spin-1 Bose-Einstein condensate, *Nat. Commun.* **3**, 1169 (2012).
- [63] E. Nicklas, M. Karl, M. Höfer, A. Johnson, W. Muessel, H. Strobel, J. Tomkovič, T. Gasenzer, and M. K. Oberthaler, Observation of Scaling in the Dynamics of a Strongly Quenched Quantum Gas, *Phys. Rev. Lett.* **115**, 245301 (2015).
- [64] K. Murata, H. Saito, and M. Ueda, Broken-axisymmetry phase of a spin-1 ferromagnetic Bose-Einstein condensate, *Phys. Rev. A* **75**, 013607 (2007).
- [65] J. Goldstone, Field theories with «Superconductor» solutions, *Nuovo Cimento* **19**, 154 (1961).
- [66] B. Damski, The Simplest Quantum Model Supporting the Kibble-Zurek Mechanism of Topological Defect Production: Landau-Zener Transitions from a New Perspective, *Phys. Rev. Lett.* **95**, 035701 (2005).
- [67] See Supplemental Material at <http://link.aps.org/supplemental/10.1103/PhysRevLett.116.155301> for a detailed discussion of the experimental methods, theory, and numerical simulations.